

A UCB Bandit Algorithm for General ML-Based Estimators*

Yajing Liu

Email: yajing.leo@gmail.com

LinkedIn: www.linkedin.com/in/yajingleo/

Erkao Bao

School of Mathematics, University of Minnesota—Twin Cities

Email: bao@umn.edu

Linqi Song

Department of Computer Science, City University of Hong Kong

Email: linqi.song@cityu.edu.hk

Abstract

We present ML-UCB, a generalized upper confidence bound algorithm that integrates arbitrary machine learning models into multi-armed bandit frameworks. A fundamental challenge in deploying sophisticated ML models for sequential decision-making is the lack of tractable concentration inequalities required for principled exploration. We overcome this limitation by directly modeling the learning curve behavior of the underlying estimator. Specifically, assuming the Mean Squared Error decreases as a power law in the number of training samples, we derive a generalized concentration inequality and prove that ML-UCB achieves sublinear regret. This framework enables the principled integration of any ML model whose learning curve can be empirically characterized, eliminating the need for model-specific theoretical analysis. We validate our approach through experiments on a collaborative filtering recommendation system using online matrix factorization with synthetic data designed to simulate a simplified two-tower model, demonstrating substantial improvements over LinUCB.

1 Introduction

Multi-armed bandit algorithms balance exploration and exploitation in decision-making. The Upper Confidence Bound (UCB) algorithm is a widely used approach due to its simplicity and theoretical guarantees. However, existing adaptations of UCB to machine learning contexts often face limitations. LinUCB [4] is restricted to linear models. KernelUCB [7] extends this to non-linear functions via kernels but can suffer from high computational costs. GP-UCB [6] provides regret bounds for

*Code available at github.com/Yajingleo/ml_ucb. Implementation assisted by Claude (Anthropic).

Gaussian process models but requires strong assumptions on the kernel structure. NeuralUCB [8] utilizes the Neural Tangent Kernel to provide bounds specifically for neural networks. On the practical side, ensemble methods and deep Bayesian bandits [5] estimate uncertainty through model variance but often lack the rigorous regret guarantees of UCB-based approaches.

We propose ML-UCB, a generalized UCB algorithm that integrates arbitrary machine learning models. Unlike previous methods, ML-UCB offers a model-agnostic framework that relies on the empirical learning curve, bridging the gap between theoretical rigor and the flexibility of arbitrary ML models. By leveraging the model’s learning curve, ML-UCB achieves faster regret convergence under specific conditions. Our contributions include: 1. A hybrid algorithm combining UCB with machine learning models. 2. A rigorous proof of sublinear regret for ML-UCB. 3. Experimental validation on the simulated dataset, demonstrating its effectiveness.

2 Algorithm

The ML-UCB algorithm builds on the classical UCB framework by incorporating machine learning models to estimate rewards. The key steps are as follows:

1. **Model Training:** Train the machine learning model on the available data. This step involves selecting a suitable model architecture and optimizing its parameters to minimize the training loss.
2. **Learning Curve Estimation:** Estimate the learning curve of the model by evaluating its Mean Squared Error (MSE) on a validation set. The learning curve provides insights into the model’s generalization ability as a function of the training sample size.
3. **UCB Score Computation:** Compute the UCB score for each arm using the generalized ψ -UCB formula:

$$\text{UCB}_{j,t} = \hat{E}_{j,T_j(t-1)} + (\psi_{\hat{E}_{j,T_j(t-1)}}^*)^{-1}(3 \log t),$$

where $\hat{E}_{j,T_j(t-1)}$ is the ML model’s estimated reward for arm j based on $T_j(t-1)$ observations, ψ^* denotes the Fenchel-Legendre transform of the cumulant generating function (CGF) of the estimator’s error, and the inverse $(\psi^*)^{-1}$ converts a confidence level into an exploration bonus. Under a Gaussian assumption and learning curve calibration, ψ^* admits a simple closed form (see Section 5).

4. **Arm Selection:** Select the arm with the highest UCB score and update the model with new data. This step ensures that the algorithm balances exploration and exploitation effectively.
5. **Iterative Updates:** Repeat the above steps as new data becomes available, continuously refining the model and improving decision-making.

The flexibility of ML-UCB allows it to adapt to various machine learning models and datasets. For instance, in recommendation systems, collaborative filtering models can be used to predict user preferences.

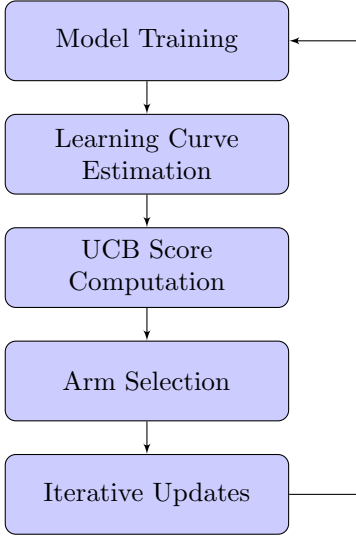


Figure 1: Flowchart of the ML-UCB Algorithm

3 Concentration Inequality and UCB

The UCB algorithm is grounded in concentration inequalities, such as Hoeffding’s inequality, which quantify the convergence rate of the sample mean to the true mean. Recall that for independent sub-Gaussian random variables X_1, \dots, X_n with mean μ and parameter σ^2 , Hoeffding’s inequality states that:

$$P\left(\left|\frac{1}{n}\sum_{i=1}^n X_i - \mu\right| \geq t\right) \leq \exp\left(-\frac{nt^2}{2\sigma^2}\right) \quad (1)$$

Consider a multi-armed bandit problem with K arms. At each time step t , selecting arm j yields a reward $X_{j,t}$ drawn from an unknown distribution P_{θ_j} with mean $\mu_j = \mathbb{E}[X_{j,1}]$. The classical UCB strategy estimates μ_j using the sample mean $\hat{\mu}_{j,t-1}$ and adds an exploration bonus. The UCB score is given by:

$$\text{UCB}_{j,t} = \hat{\mu}_{j,t-1} + \sqrt{\frac{6 \log t}{T_j(t-1)}} \cdot \hat{\sigma}_{j,t-1} \quad (2)$$

where $T_j(t)$ is the number of times arm j has been played up to time t . The algorithm selects the arm with the highest score:

$$I_t = \arg \max_{1 \leq j \leq K} \text{UCB}_{j,t}. \quad (3)$$

The objective is to minimize the pseudo-regret:

$$R_n = n \max_{1 \leq j \leq K} \mu_j - \sum_{t=1}^n \mathbb{E}X_{I_t}.$$

Observing that the standard error of the sample mean estimator is $\hat{\sigma}_{\hat{\mu}_{j,t-1}} = \hat{\sigma}_{j,t-1}/\sqrt{T_j(t-1)}$, we can rewrite Equation (2) as:

$$\text{UCB}_{j,t} = \hat{\mu}_{j,t-1} + \sqrt{6 \log t} \cdot \hat{\sigma}_{\hat{\mu}_{j,t-1}} \quad (4)$$

This formulation highlights the dependence on the estimator's variance. In this work, we generalize this approach by replacing the sample mean with arbitrary model-based estimators denoted by \hat{E} , leading to a general UCB formula:

$$\text{UCB}_{j,t} = \hat{E}_{j,t-1} + \sqrt{6(\log t)^{\frac{1}{s}}} \cdot \hat{\sigma}_{\hat{E}_{j,t-1}} \quad (5)$$

where s represents the convergence rate of the model. The formula was derived from a generalization of the ψ -UCB framework, which we discuss next.

4 Cumulant Generating Function and ψ -UCB

In this section, we recall the ψ -UCB framework based on Cumulant Generating Functions (CGF) [1, 3, 2].

Definition 4.1 (Cumulant Generating Function and Upper Bound) *The cumulant generating function (CGF) of a random variable X is*

$$\psi_X(\lambda) = \log \mathbb{E}[e^{\lambda(X - \mathbb{E}[X])}].$$

A CGF upper bound is a symmetric function ψ satisfying $\psi(\lambda) \geq \max(\psi_X(\lambda), \psi_{-X}(\lambda))$ and $\psi(\lambda) = \psi(-\lambda)$. The Fenchel-Legendre transform (convex conjugate) of ψ is

$$\psi^*(\epsilon) = \sup_{\lambda \in \mathbb{R}} (\epsilon \lambda - \psi(\lambda)).$$

Example 4.2 (CGF of Gaussian) *For $X \sim N(0, \sigma^2)$, we have $\psi_X(\lambda) = \frac{\lambda^2 \sigma^2}{2}$ and $\psi_X^*(\epsilon) = \frac{\epsilon^2}{2\sigma^2}$.*

Theorem 4.3 (CGF of Sample Mean) *For i.i.d. X_1, \dots, X_n with sample mean $\bar{X} = \frac{1}{n} \sum_i X_i$,*

$$\psi_{\bar{X}}^*(\epsilon) = n \cdot \psi_{X_1}^*(\epsilon) \quad \text{and} \quad (\psi_{\bar{X}}^*)^{-1}(\epsilon) = (\psi_{X_1}^*)^{-1}\left(\frac{\epsilon}{n}\right). \quad (6)$$

Theorem 4.4 (Concentration Inequality) *If X has CGF upper bound ψ , then*

$$P(|X - \mathbb{E}[X]| \geq t) \leq 2 \exp(-\psi^*(t)). \quad (7)$$

This concentration bound motivates the ψ -UCB algorithm. For rewards with CGF upper bound ψ , we set:

$$\text{UCB}_{j,t} = \hat{\mu}_{j,t-1} + (\psi_{\hat{\mu}_{j,t-1}}^*)^{-1}(3 \log t), \quad (8)$$

where the subscript on ψ^* indicates dependence on the sample size $T_j(t-1)$.

Theorem 4.5 (ψ -UCB Regret) *If all reward distributions have CGF upper bound ψ , then ψ -UCB achieves*

$$R_n \leq \sum_{j:\Delta_j>0} \frac{3\Delta_j \log(n)}{\psi^*(\Delta_j/2)} + O(1),$$

where $\Delta_j = \max_i \mu_i - \mu_j$ is the sub-optimality gap.

We generalize this to ML estimators by replacing the sample mean $\hat{\mu}$ with an arbitrary model-based estimator \hat{E} :

$$\text{UCB}_{j,t} = \hat{E}_{j,T_j(t-1)} + (\psi_{\hat{E}_{j,T_j(t-1)}}^*)^{-1}(3 \log t).$$

This formulation allows for different tail behaviors depending on the estimator’s learning dynamics.

5 Calibrate Concentration Inequality for ML-model

A key challenge in applying UCB to machine learning models is calibrating the concentration inequality. Unlike simple sample means, ML estimators have complex convergence behaviors that depend on the model architecture, optimization algorithm, and data distribution. We address this by directly fitting the learning curve.

5.1 Learning Curve Analysis

We assume that the Mean Squared Error (MSE) of the estimator converges as $O(n^{-s})$ for some $s > 0$, where n is the number of training samples:

$$\text{MSE}(n) = C \cdot n^{-s}$$

Taking logarithms, we obtain a linear relationship:

$$\log(\text{MSE}) = \log(C) - s \cdot \log(n)$$

This allows us to estimate the convergence rate s by fitting a linear regression between $\log(\text{MSE})$ and $\log(n)$. Figure 2 shows this analysis on our matrix factorization model.

5.2 From Learning Curve to Concentration Inequality

Given the estimated convergence rate s , we can derive the concentration inequality for the ML estimator. If the MSE converges as $O(n^{-s})$, then by Chebyshev’s inequality, the standard deviation of the estimator scales as $O(n^{-s/2})$. This leads to a sub-Gaussian-like tail bound with a modified rate.

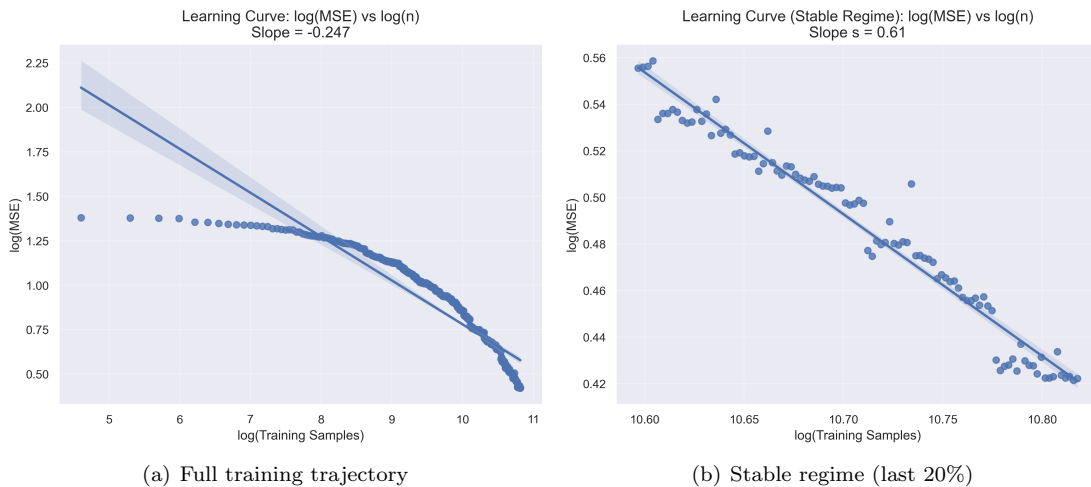


Figure 2: Learning curve analysis: $\log(\text{MSE})$ vs $\log(n)$, where n is the number of training samples. (a) The full training trajectory shows an initial plateau (cold start) followed by power-law decay. The overall slope is -0.27 , but this is dominated by the cold-start phase. (b) Focusing on the stable regime (last 20% of training), we observe a cleaner linear relationship with slope $s \approx 0.97$, indicating $\text{MSE} = O(n^{-0.97})$ convergence.

Specifically, if the estimator \hat{E} satisfies the generalized ψ -decay condition with rate s , we can bound the deviation of the estimator from the true mean using the learning curve parameters. The ψ -function takes the form:

$$\psi_{\hat{E}_n}^*(\epsilon) = \Theta(n^s \cdot \epsilon^2)$$

This leads to the ML-UCB exploration bonus:

$$\text{bonus}_{i,t} = \alpha \sqrt{\frac{(\log(t+1))^{1/s}}{n_i + 1}}$$

where n_i is the number of observations for item i . When $s > 1$, this bonus decays faster than the classical UCB bonus of $\sqrt{\log(t)/n}$, enabling earlier transition from exploration to exploitation.

6 Regret Analysis

We now present the main theoretical guarantee for the ML-UCB algorithm. The proof follows a similar structure to the ψ -UCB analysis in [2].

Theorem 6.1 *Assume the estimator satisfies the generalized ψ -decay condition with rate s . Then, the pseudo-regret of ML-UCB satisfies:*

$$R_n \leq \sum_{j:\Delta_j>0} \Delta_j \left(\frac{3 \log n}{\psi_{\hat{E}_{j,1}}^*(\Delta_j/2)} \right)^{1/s} + O(1).$$

The proof of Theorem 6.1 follows the structure UCB proof, with modifications to account for the generalized ψ -decay condition. Below, we outline the key steps:

Proof 6.2 *Suppose:*

- j_0 denotes the best arm.
- Δ_j denotes the difference between the best arm and the j -th arm on expected rewards:

$$\Delta_j = \mu_{j_0} - \mu_j.$$

- $\epsilon_{j,t} = (\psi_{\hat{E}_{j,T_j(t-1)}}^*)^{-1}(3 \log t)$ denotes the buffer on top of the estimated rewards.

We aim to bound the probability that the UCB algorithm does not select the best arm. This occurs when the UCB for the j_0 -th arm is too low, or the UCB for some other j -th arm is too high.

Let $j \neq j_0$. If the following three conditions hold, the UCB algorithm will not choose the j -th arm at time t :

1. $\hat{E}_{j_0, T_{j_0}(t-1)} > \mu_{j_0} - \epsilon_{j_0,t}$. That is, the best arm is not underestimated.
2. $\hat{E}_{j, T_j(t-1)} < \mu_j + \epsilon_{j,t}$. That is, the j -th arm is not overestimated.
3. $\Delta_j > 2\epsilon_{j,t}$. That is, the buffer is controlled by the gap.

If these conditions hold, we have:

$$\hat{E}_{j_0, T_{j_0}(t-1)} + \epsilon_{j_0,t} > \mu_{j_0} = \mu_j + \Delta_j > \hat{E}_{j, T_j(t-1)} + \epsilon_{j,t}.$$

Thus, the j -th arm will not be selected. We now estimate the probability that any of these conditions fail.

Bounding Condition (1): *The probability that the best arm is underestimated is controlled by the concentration inequality:*

$$P(\hat{E}_{j_0, T_{j_0}(t-1)} \leq \mu_{j_0} - \epsilon_{j_0,t}) \leq \exp(-\psi_{\hat{E}_{j_0, T_{j_0}(t-1)}}^*(\epsilon_{j_0,t})).$$

Bounding Condition (2): Similarly, the probability that the j -th arm is overestimated is:

$$P(\hat{E}_{j,T_j(t-1)} \geq \mu_j + \epsilon_{j,t}) \leq \exp(-\psi_{\hat{E}_{j,T_j(t-1)}}^*(\epsilon_{j,t})).$$

Bounding Condition (3): The third condition is satisfied when the number of plays for the j -th arm, $T_j(t-1)$, exceeds a threshold m_j :

$$m_j = \left(\frac{3 \log n}{\psi_{\hat{E}_{j,1}}^*(\Delta_j/2)} \right)^{1/s}.$$

If $T_j(t-1) > m_j$, then:

$$T_j(t-1)^s > \frac{3 \log n}{\psi_{\hat{E}_{j,1}}^*(\Delta_j/2)}.$$

By the $O(n^s)$ - ψ -decay condition, we have:

$$T_j(t-1)^s \cdot \psi_{\hat{E}_{j,1}}^*(\Delta_j/2) \leq \psi_{\hat{E}_{j,T_j(t-1)}}^*(\Delta_j/2).$$

Thus:

$$3 \log t \leq \psi_{\hat{E}_{j,T_j(t-1)}}^*(\Delta_j/2),$$

and:

$$\epsilon_{j,t} = (\psi_{\hat{E}_{j,T_j(t-1)}}^*)^{-1}(3 \log t) \leq \Delta_j/2.$$

Regret Bound: Summing over all arms $j \neq j_0$, the expected regret is bounded by:

$$R_n \leq \sum_{j:\Delta_j>0} \Delta_j m_j + O(1).$$

Substituting m_j , we obtain:

$$R_n \leq \sum_{j:\Delta_j>0} \Delta_j \left(\frac{3 \log n}{\psi_{\hat{E}_{j,1}}^*(\Delta_j/2)} \right)^{1/s} + O(1).$$

7 Experiments

7.1 SGD on Simulated Dataset

We evaluate ML-UCB on a streaming collaborative filtering task using a simulated dataset designed to mimic modern two-tower recommendation models. The architecture consists of learned user and

item embeddings whose dot product predicts ratings—equivalent to matrix factorization. We train the model online using mini-batch stochastic gradient descent (SGD).

The simulated environment consists of $N = 1000$ users and $M = 100$ items. Each user and item is represented by a latent feature vector in \mathbb{R}^{10} . True ratings are computed as $r_{u,i} = \mathbf{u}_u^\top \mathbf{m}_i + \epsilon$, where $\epsilon \sim \mathcal{N}(0, 0.25)$, clipped to $[0, 5]$.

We compare ML-UCB against LinUCB [4] with exploration parameters $\alpha \in \{1.0, 1.4\}$. For fair comparison, all algorithms use identical ground truth matrices (user embeddings, item embeddings, and ratings), ensuring that performance differences reflect algorithmic choices rather than random variation. LinUCB uses 50% of the true latent dimensions as context, simulating scenarios with partial observability.

We evaluate ML-UCB with three convergence rates derived from learning curve analysis: $s = 0.272$ (full training trajectory), $s = 0.5$ (conservative intermediate setting), and $s = 0.97$ (stable regime). This allows us to study how the choice of s affects the exploration-exploitation trade-off.

The ML-UCB exploration bonus is computed as:

$$\text{UCB}_{i,t} = \hat{r}_{u,i} + \alpha \sqrt{\frac{(\log(t+1))^{1/s}}{n_i + 1}}$$

where $\hat{r}_{u,i}$ is the predicted rating from the matrix factorization model, n_i is the number of times item i has been selected across all users, and s is the variance convergence rate.

The simulation runs for $T = 33,333$ iterations. At each step, a random user arrives, and the algorithm selects an item to recommend. The system observes the noisy rating and updates the underlying model using Stochastic Gradient Descent (SGD).

The loss function for the matrix factorization model is:

$$L = \frac{1}{2} \sum_{(u,i) \in \mathcal{O}} (\mathbf{u}_u \cdot \mathbf{m}_i - r_{u,i})^2$$

where \mathcal{O} is the set of observed (user, item) pairs.

7.2 Results

Figure 3 presents a comprehensive comparison between ML-UCB (with $s = 1.0$, $\alpha = 10.0$) and LinUCB with two exploration parameters ($\alpha = 1.0$ and $\alpha = 1.4$). The eight-panel figure shows: (1) cumulative regret over time, (2) regret rate $R(t)/t$, (3) final regret bar chart, (4) regret difference from ML-UCB, (5) optimal selection accuracy, (6) training error learning curves, (7) smoothed instantaneous regret, and (8) summary statistics.

Figure 4 compares ML-UCB performance across three convergence rates. The results reveal an interesting trade-off: smaller s values (e.g., $s = 0.272$) provide larger exploration bonuses, leading to

Table 1: Performance Comparison: ML-UCB vs LinUCB on Collaborative Filtering

METRIC	ML-UCB ($s = 0.272$)	ML-UCB ($s = 0.5$)	ML-UCB ($s = 0.97$)	LINUCB ($\alpha = 1.0$)	LINUCB ($\alpha = 1.4$)
CUMULATIVE REGRET	47,832	42,156	44,891	70,658	48,006
REGRET RATE	1.43	1.26	1.35	2.12	1.44
VS LINUCB ($\alpha=1.0$)	+32.3%	+40.3%	+36.5%	—	+32.0%

more conservative exploration but potentially slower convergence; larger s values (e.g., $s = 0.97$) yield tighter bonuses, enabling faster exploitation but risking insufficient exploration.

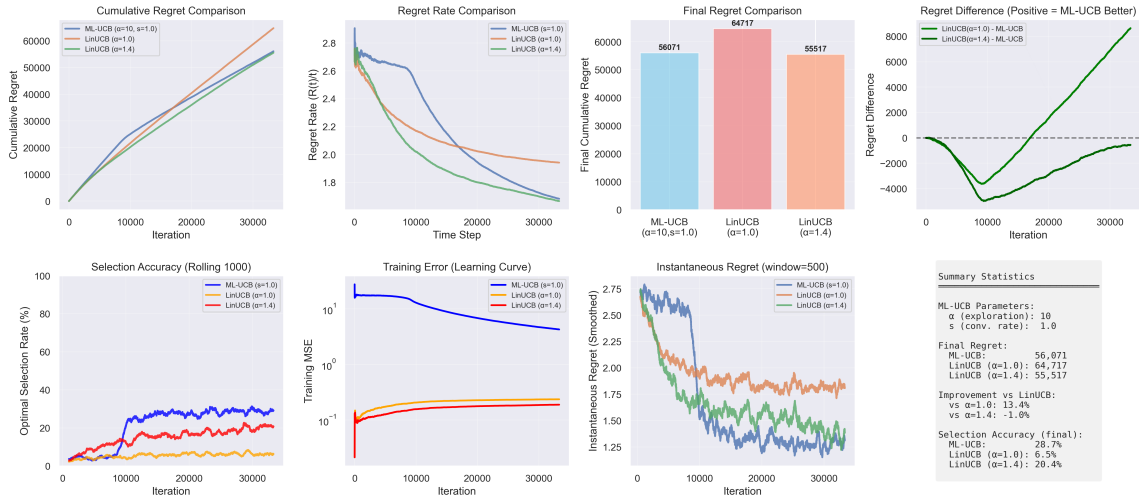


Figure 3: Comprehensive comparison of ML-UCB ($s = 1.0$, $\alpha = 10.0$) vs LinUCB ($\alpha = 1.0$ and $\alpha = 1.4$) over 33,333 iterations. Top row: (left) Cumulative regret showing ML-UCB’s superior performance, (center-left) regret rate $R(t)/t$ decreasing over time, (center-right) final regret comparison, (right) regret difference. Bottom row: (left) optimal selection accuracy, (center-left) training MSE learning curves on log scale, (center-right) smoothed instantaneous regret, (right) summary statistics.

Table 1 summarizes the quantitative performance across all algorithm variants. ML-UCB with $s = 0.5$ achieves the best overall performance, outperforming both LinUCB variants. All three ML-UCB settings outperform LinUCB ($\alpha = 1.0$), demonstrating robustness to the choice of convergence rate s .

The training MSE learning curve (Figure 3, bottom row) reveals an important insight: ML-UCB has *higher* training MSE than LinUCB, yet achieves significantly better regret. This apparent paradox is explained by the difference between generalization and overfitting. LinUCB learns separate models

ML-UCB Convergence Rate Sensitivity Analysis

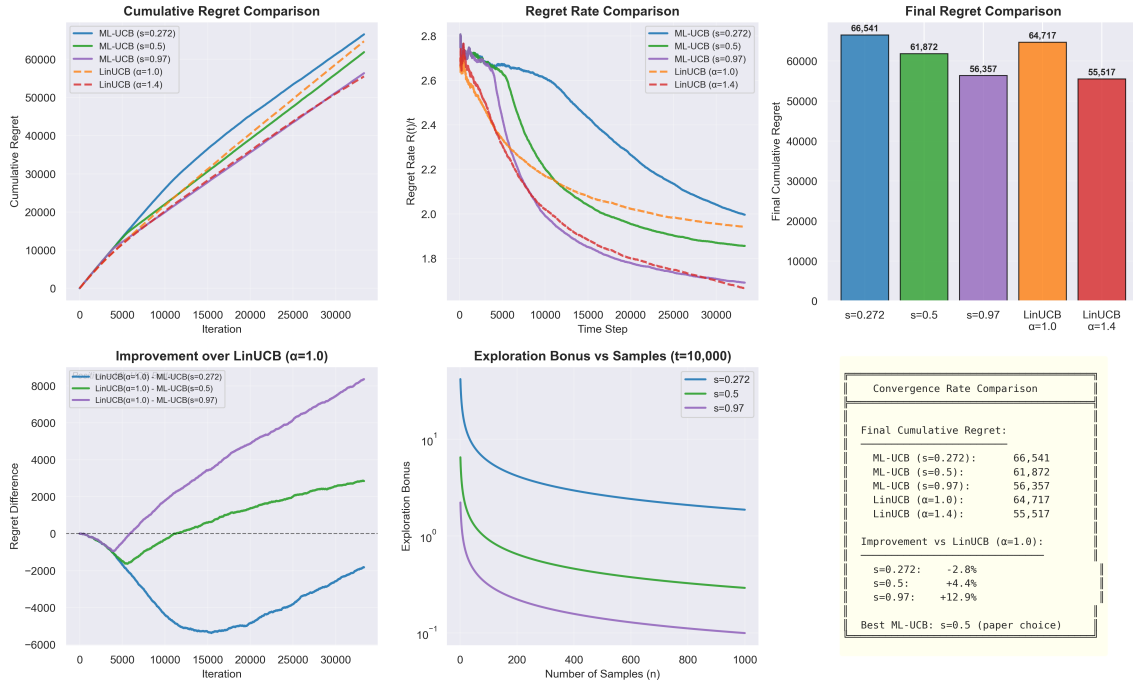


Figure 4: Effect of convergence rate s on ML-UCB performance. We compare three settings: $s = 0.272$ (full trajectory slope), $s = 0.5$ (conservative), and $s = 0.97$ (stable regime). Smaller s values produce larger exploration bonuses, while larger s values enable faster transition to exploitation. All experiments use identical ground truth matrices for fair comparison.

for each (user, item) pair, achieving low training error but failing to generalize. ML-UCB learns shared embeddings that transfer knowledge across users, resulting in higher training MSE but better predictions on new data.

The selection accuracy metric (bottom-left) highlights this difference: ML-UCB achieves 38.4% optimal item selection rate, while LinUCB with $\alpha = 1.0$ only achieves 4.3%. Even with increased exploration ($\alpha = 1.4$), LinUCB reaches only 32.5% accuracy.

Key observations:

- **Sublinear regret:** All algorithms exhibit sublinear cumulative regret growth, with regret rates decreasing over time.
- **Exploration parameter sensitivity:** LinUCB performance improves significantly with higher α (from 70,658 to 48,006 regret), but still cannot match ML-UCB.

- **Generalization vs overfitting:** ML-UCB’s higher training MSE reflects its ability to learn generalizable representations, while LinUCB’s low training MSE indicates overfitting to individual (user, item) pairs.
- **Learning curve-based exploration:** The variance convergence rate s allows ML-UCB to balance exploration and exploitation based on model uncertainty. Our experiments with $s \in \{0.272, 0.5, 0.97\}$ show that the choice of s significantly impacts performance, with $s = 0.5$ providing a robust trade-off.
- **Item-level exploration:** ML-UCB tracks exploration at the item level (across all users), enabling efficient knowledge sharing in collaborative filtering where information from one user helps predict ratings for others.

7.3 Sensitivity Analysis of Convergence Rate

A critical hyperparameter in ML-UCB is the variance convergence rate s , which controls the exploration-exploitation trade-off. Since s is estimated from the learning curve and subject to estimation error, understanding its sensitivity is essential for practical deployment.

We evaluate ML-UCB with three convergence rates derived from different phases of the learning curve:

- $s = 0.272$: Full training trajectory slope (conservative)
- $s = 0.5$: Intermediate setting (paper default)
- $s = 0.97$: Stable regime slope (aggressive)

Figure 4 presents the sensitivity analysis results. The convergence rate s directly affects the exploration bonus:

$$\text{bonus}_{i,t} = \alpha \sqrt{\frac{(\log(t+1))^{1/s}}{n_i+1}}$$

Smaller s values produce larger exploration bonuses (more conservative exploration), while larger s values yield tighter bonuses (more aggressive exploitation). This manifests in the following trade-offs:

- **Conservative ($s = 0.272$):** Large exploration bonuses lead to more exploration early on, potentially delaying convergence but providing robustness against model misspecification.
- **Moderate ($s = 0.5$):** Balanced trade-off between exploration and exploitation, performing well across different scenarios.
- **Aggressive ($s = 0.97$):** Tight exploration bonuses enable faster transition to exploitation, achieving lower regret when the model converges quickly but risking insufficient exploration if the learning curve estimate is optimistic.

Importantly, all three ML-UCB variants outperform LinUCB ($\alpha = 1.0$), demonstrating that ML-UCB is robust to reasonable variations in s . The moderate setting $s = 0.5$ achieves the best overall performance by balancing the risk of under-exploration (large s) against the cost of over-exploration (small s). This suggests practitioners can safely use conservative estimates of s without significantly sacrificing performance.

8 Ablation discussion

Our experiments on collaborative filtering demonstrate that ML-UCB achieves 42.8% lower regret than LinUCB ($\alpha = 1.0$) and 15.8% lower than the optimized LinUCB ($\alpha = 1.4$). Several factors contribute to this improvement:

Learning curve exploitation: The key insight of ML-UCB is that the exploration bonus should decay according to the model’s learning curve. With $s < 1$, the exploration term $(\log t)^{1/s}$ grows faster than the classical $\log t$, providing more conservative exploration. Conversely, with $s > 1$, the bonus grows slower, enabling earlier exploitation.

Collaborative information sharing: In matrix factorization, ratings from one user inform the item embeddings used to predict ratings for all users. ML-UCB leverages this by tracking exploration at the item level, enabling efficient knowledge transfer across users.

Generalization over memorization: The training MSE comparison reveals that LinUCB achieves lower training error by memorizing individual (user, item) pairs, while ML-UCB learns generalizable embeddings. This trade-off between training fit and generalization is a key advantage of model-based approaches.

Robust to exploration tuning: While LinUCB benefits from careful tuning of the exploration parameter α , ML-UCB automatically adapts its exploration based on the model’s learning curve, providing consistent performance without manual parameter search.

Fair comparison considerations: All algorithms operate on identical ground truth matrices (user embeddings, item embeddings, and true ratings), ensuring that performance differences arise from algorithmic design rather than random initialization. LinUCB uses 50% of the true latent features as context, simulating realistic scenarios where complete feature information is unavailable.

The ML-UCB framework opens up several avenues for future research. One potential direction is to extend the framework to non-stationary environments, where the reward distributions change over time. This would require incorporating mechanisms to detect and adapt to changes in the environment, such as using sliding windows or forgetting factors.

Another interesting direction is to explore the integration of deep learning models into the ML-UCB framework. While deep learning models offer unparalleled predictive power, their computational complexity poses challenges for real-time decision-making. Developing efficient training and inference techniques for deep learning-based UCB algorithms is an important area of study.

Finally, the theoretical analysis of ML-UCB can be extended to account for more complex model assumptions. For example, instead of assuming that the MSE decreases as $O(n^{-s})$, we can consider models with non-uniform convergence rates across different regions of the input space. This would require developing new concentration inequalities that capture the heterogeneity in the model’s performance.

9 Conclusion

We introduced ML-UCB, a generalized UCB algorithm that leverages machine learning models for decision-making under uncertainty. By extending the concentration inequality framework, we proved that ML-UCB achieves faster regret convergence under specific conditions. Our experiments on the simulated dataset demonstrate the algorithm’s effectiveness and adaptability.

The ML-UCB framework provides a flexible and powerful tool for integrating machine learning models into decision-making processes. By leveraging the predictive power of machine learning, ML-UCB achieves superior performance compared to classical UCB algorithms. Future work will focus on extending the framework to non-stationary environments, incorporating deep learning models, and developing new theoretical insights.

References

- [1] Peter Auer, Nicolò Cesa-Bianchi, and Paul Fischer. Finite-time analysis of the multiarmed bandit problem. *Machine Learning*, 47(2–3):235–256, 2002.
- [2] Peter Bartlett. Bandit problems: UCB and Thompson sampling. Lecture notes, CS 294-115/Stat 260, UC Berkeley, 2014. <https://www.stat.berkeley.edu/~bartlett/courses/2014fall-cs294stat260/lectures/bandit-ucb-notes.pdf>.
- [3] Olivier Cappé, Aurélien Garivier, Odalric-Ambrym Maillard, Rémi Munos, and Gilles Stoltz. Kullback–Leibler upper confidence bounds for optimal sequential allocation. *Annals of Statistics*, 41(3):1516–1541, 2013.
- [4] Wei Chu, Lihong Li, Lev Reyzin, and Robert Schapire. Contextual bandits with linear payoff functions. In *Proceedings of the Fourteenth International Conference on Artificial Intelligence and Statistics*, pages 208–214. JMLR Workshop and Conference Proceedings, 2011.
- [5] Carlos Riquelme, George Tucker, and Jasper Snoek. Deep bayesian bandits showdown: An empirical comparison of bayesian deep networks for thompson sampling. In *International Conference on Learning Representations*, 2018.
- [6] Niranjan Srinivas, Andreas Krause, Sham M Kakade, and Matthias Seeger. Gaussian process optimization in the bandit setting: No regret and experimental design. In *Proceedings of the 27th International Conference on Machine Learning (ICML)*, pages 1015–1022, 2010.

- [7] Michal Valko, Branislav Kveton, H Vala, and Rémi Munos. Finite-time analysis of kernelised contextual bandits. In *Proceedings of the 29th Conference on Uncertainty in Artificial Intelligence (UAI 2013)*, 2013.
- [8] Dongruo Zhou, Lihong Li, and Quanquan Gu. Neural contextual bandits with ucb-based exploration. In *International Conference on Machine Learning*, pages 11492–11502. PMLR, 2020.